Opportunistic Access Point Selection for Mobile Edge Computing Networks

Junjuan Xia, Lisheng Fan, Nan Yang, Yansha Deng, Trung Q. Duong, George K. Karagiannidis, *Fellow, IEEE*, and Arumugam Nallanathan, *Fellow, IEEE*

***Abstract*—In this paper, we investigate a mobile edge computing (MEC) network with two computational access points (CAPs), where the source is equipped with multiple antennas and it has some computation tasks to be accomplished by the CAPs through Nakagami-m distributed wireless links. Since the MEC network involves both communication and computation, we first define the outage probability by taking into account the joint impact of latency and energy consumption. From this new definition, we then employ receiver antenna selection (RAS) or maximal ratio combining (MRC) at the receiver, and apply selection combining (SC) or switch-and-stay combining (SSC) protocol to choose a CAP to accomplish the computation task from the source. For both protocols along with the RAS and MRC, we further analyze the network performance by deriving new and easy-to-use analytical expressions for the outage probability over Nakagami-m fading channels, and study the impact of the network parameters on the outage performance. Furthermore, we provide the asymptotic outage probability in the low regime of noise power, from which we obtain some important insights on the system design. Finally, simulations and numerical results are demonstrated to verify the effectiveness of the proposed approach. It is shown that the number of transmit antenna and Nakagami parameter can help reduce the latency and energy consumption effectively, and the SSC protocol can achieve the same performance as the SC protocol with proper switching thresholds of latency and energy consumption.**

***Index Terms*—Mobile edge computing, latency, energy consumption, opportunistic selection.**

J. Xia and L. Fan are both with the School of Computer Science and Cyber Engineering, Guangzhou University, Guangzhou, China (e-mail: {xiajunjuan,lsfan}@gzhu.edu.cn).

N. Yang is with the Research School of Electrical, Energy and Materials Engineering, Australian National University, Canberra, ACT 2601, Australia (e-mail: nan.yang@anu.edu.au).

Y. Deng is with the Department of Informatics, King's College London, London WC2R 2LS, UK (e-mail: yansha.deng@kcl.ac.uk).

T. Q. Duong is with School of Electronics, Electrical Engineering and Computer Science, Queens University Belfast, Belfast BT7 1NN, U.K. (e-mail: trung.q.duong@qub.ac.uk).

G. K. Karagiannidis is with the Department of Electrical and Computer Engineering, Aristotle University of Thessaloniki, Thessaloniki 54636, Greece (e-mail: geokarag@auth.gr).

A. Nallanathan is with the School of Electronic Engineering and Computer Science, Queen Mary University of London, London, U.K (e-mail: a.nallanathan@qmul.ac.uk).

The corresponding author of this paper is Lisheng Fan.

This work was supported in part by the NSFC (No. 61871139), in part by the International Science and Technology Cooperation Projects of Guangdong Province (No. 2020A0505100060), in part by the Science and Technology Program of Guangzhou (No. 201807010103), and in part by the research program of Guangzhou University (No. YK2020008). The work of T. Q. Duong was supported in part by the Royal Academy of Engineering (RAEng) under the RAEng Research Chair and Senior Research Fellowship scheme Grant RCSRF2021\11\41 and RAEng Research Fellowships scheme Grant RF1415\14\22.

I. Introduction

With the deployment of the fifth-generation (5G) wireless networks [1]–[4], many new services and applications are introduced, such as augmented reality, autonomous driving, etc. One major characteristic of these applications is that they require intensive computations, which should be accomplished in a very fast way. Accordingly, the traditional *communication-orientated* systems have been gradually evolving into *computation-orientated* systems, and the performance metrics of interest have extended from the conventional quality such as the transmission error and data rate to latency and energy consumption [5], [6]. To support the intensive computation needs of the next-generation communication networks, the concept of mobile edge computing (MEC) has been proposed [7]–[10], where the edge nodes serve as the computational access points (CAPs) to help in accomplishing the computation tasks through wireless links. In particular, Hu *et.al* [11] investigated the edge and central cloud computing by proposing a perfect pairing for high energy efficiency and low-latency, which provides critical guidance to the research of MEC.

In MEC networks' design, the key is to take into account the joint impact of communication and computation [12]–[15]. In this direction, the authors in [16] investigated the performance of wireless powered MEC systems, by analyzing the problem of joint offloading and computing optimization, and concluded that the average energy consumption could be substantially reduced by offloading optimization. Then, the use of cooperative communications in the form of relaying can be incorporated into the wireless powered MEC systems, which can effectively reduce the transmit energy [17]. Later, multiuser MEC networks with non-orthogonal multiple access (NOMA) were studied in [18], and the computation offloading was optimized to reduce the average sum-energy. Furthermore, the impact of NOMA on the offloading of MEC networks was studied in [19], and it was found that the system performance could be significantly improved by using offloading optimization. Finally, by incorporating caching into MEC networks for 5G communication systems, a deep reinforcement learning based approach could be used to intelligently optimize the network resources [20].

To improve the performance of MEC networks, opportunistic selection can be applied as a powerful candidate to assist the communication and computation. For wireless networks with multiple relays, selection combining (SC) can be performed to select the best relay branch in order to exploit the channel fluctuations among relays [21]. When multiple

antennas are equipped at the source in the SC-based relaying networks, the technique of transmit antenna selection (TAS) or maximal ratio transmission (MRT) can be utilized to assist the data transmission [22], [23]. Similarly, when multiple antennas are equipped at the destination in the SC-based relaying networks, the technique of receiver antenna selection (RAS) or maximal ratio combining (MRC) can be used [24], [25]. However, the SC protocol requires to continuously estimate the channel parameters of all branches at the beginning of each block transmission, which imposes a big load on the system implementation. Another limitation is that it may result in frequent branch switching, which is harmful to the network stability. To overcome these limitations, switching-and-stay combining (SSC) protocol is employed to achieve a balance between performance and implementation complexity. According to SSC, the same branch continues to be used as long as the signal-to-noise ratio (SNR) is above a certain threshold [26]–[28]. Also, for relaying networks with available direct links, distributed SSC can be used to exploit the benefits of both relaying and direct links, without increasing the implementation complexity [29]–[31].

In this paper, we study the opportunistic CAP selection for MEC networks with two CAPs, where the CAPs are equipped with multiple antennas and they can accomplish the computation tasks from the source. We start with the critical question: "What is the definition of the outage probability in MEC networks?". To answer this question, we define the outage probability by taking into account both latency and energy consumption, from the perspectives of communication and computation, respectively. In order to improve the network outage performance, we then apply RAS or MRC at the receiver, and employ two opportunistic selection protocols, i.e., SC and SSC, to choose a CAP to accomplish the computation tasks. We proceed with the important question: "What is the effect of the system parameters on the MEC networks design?". To tackle this problem, we study the system performance of the SC-based and SSC-based MEC networks, by deriving analytical and asymptotic expressions for the outage probability. We further analyze how the outage probability varies with the network parameters, from which we obtain some important insights on the system design. Simulations and numerical results are finally demonstrated to verify the proposed analysis.

The key contributions of this paper are summarized as follow:

- We define a new form of outage probability by taking into account both latency and energy consumption, from the perspectives of communication and computation.
- We employ the RAS or MRC at the receiver, and then apply the SC or SSC protocol to choose a CAP to accomplish the computation tasks, in order to improve the network outage performance of the MEC networks.
- We derive analytical and asymptotic expressions for the outage probabilities of the MEC networks, in order to investigate the outage performance achieved by the SC and SSC protocols.
- We obtain some important insights on the system design, by analyzing how the outage probability varies with the network parameters. In particular, the number of transmit antenna and Nakagami parameter can help reduce the latency and energy consumption rapidly, and the SSC protocol can achieve the same performance as the SC protocol with proper branch switching thresholds of latency and energy consumption.

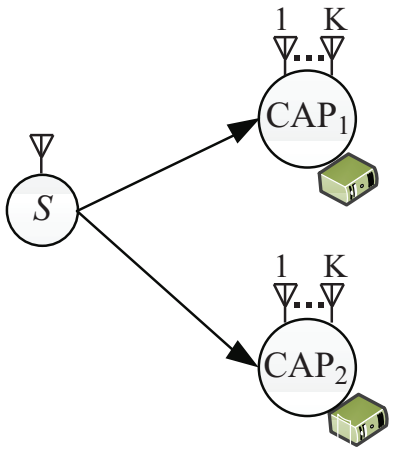

Fig. 1. System model of a MEC network consisting of one user and two CAPs equipped with multiple antennas.

The organization of this paper is as follows. After the introduction, Section II describes the model of MEC networks with two CAPs. Section III presents a new definition of the outage probability in MEC networks, and Section IV provides the SC and SSC protocols for the MEC networks. Section V provides the analytical and asymptotic outage probability expressions for the two protocols. Numerical results are provided in Section VI to offer valuable insights into the outage performance, and finally, conclusions are drawn in Section VII.

Notations: Let $\mathcal{CN}(0,\beta)$ be a random variable (RV) with zero mean and variance β, subject to circularly symmetric complex Gaussian. We denote $\text{Nak}(m,\alpha)$ as Nakagami-m distribution with the parameter m and variance α. In addition, we use $f_X(\cdot)$ to denote the probability density function (PDF) of the RV X, and the operation $\Pr(\cdot)$ returns probability.

II. Network Model

Fig. 1 illustrates a MEC network with one user and two CAPs $\{\text{CAP}_i|i=1,2\}$[1], where the source (user) is equipped with a single antenna while the CAPS are equipped with K antennas. The source S has some computation tasks but does not have the computational ability to perform them. Thus, S requests the help from the two CAPs through wireless links subject to Nakagami-m fading. Note that Nakagami-m fading is a generalized fading model and it fits well in practical communication scenarios, such as indoor and land-mobile communications [31]. Let $\mathbf{h}_1 = [h_{1,1},\cdots,h_{1,K}]$ and $\mathbf{h}_2 = [h_{2,1},\cdots,h_{2,K}]$ denote the channel vectors of the wireless links S-CAP_1 and S-CAP_2, where each element in the vector

[1]If there are more than two CAPs in the network, the SC and SSC protocols can be extended, and the derivation process in this paper can be readily applied in a straightforward way.

follows Nakagami-m distribution, i.e., $h_{1,k} \sim \text{Nak}(m_1, \alpha_1)$ and $h_{2,k} \sim \text{Nak}(m_2, \alpha_2)$ with $k \in \{1, \cdots, K\}$. Note that we consider one user in the MEC network of this paper, and if there are multiple users existing in the system, user scheduling can be used to enhance the system reliability performance, based on the system parameters such as the instantaneous channel coefficients. The study of the MEC network with a single user in this work is meaningful, since it can provide a useful reference for the MEC network with multiple users. In addition, adding multiple users into this work would somewhat change the focus of this work, which is the AP selection and diversity reception. In our future work, we will investigate the MEC network with multiple users, and incorporate the user scheduling into the considered system.

Suppose that each computation task at the source contains L bits[2], and the CAP with number i (CAP_i) is selected for computation. Then, the latency of the wireless transmission is given by,

$$t_{i1} = \frac{L}{W_B \log_2(1 + \frac{P_S}{\sigma^2} u_i)}, \tag{1}$$

where W_B is the channel bandwidth, P_S is the transmit power of S, and σ^2 is the noise variance of the additive white Gaussian noise (AWGN) at the CAP. We use u_i to denote the instantaneous channel gain of the S-CAP_i link. Specifically, when the RAS is employed at the receiver, u_i is given by

$$u_i = \max_{1 \le k \le K} |h_{i,k}|^2. \tag{2}$$

When the MRC is employed at the reeiver, u_i is given by

$$u_i = ||\mathbf{h}_i||^2. \tag{3}$$

After the CAP_i receives and computes the task, the computation latency is,

$$t_{i2} = \frac{\rho L}{f_i}, \tag{4}$$

where ρ is the number of required CPU cycles for each bit and f_i is the CPU-cycle frequency at the CAP_i. For the bit-wise independent computation task, the computation can start without having to wait for the transmission end of the whole task. On the contrary, for the bit-wise dependent computation task, the computation cannot start until the transmission end of the whole task. Some practical examples of the bit-wise dependent computation task are image processing based or matrix computation based tasks. In this work, we adopt the bit-wise dependent task and thus, the computation has to wait until the transmission end of the task. Accordingly, the system latency is the sum of the transmission latency and computation latency. Hence, from (1) and (4), the latency and energy consumption of both communication and computation when CAP_i is used are given by

$$t_i = \frac{L}{W_B \log_2(1 + \frac{P_S}{\sigma^2} u_i)} + \frac{\rho L}{f_i}, \tag{5}$$

$$E_i = \frac{L P_S}{W_B \log_2(1 + \frac{P_S}{\sigma^2} u_i)} + \frac{\rho L P_{c,i}}{f_i}, \tag{6}$$

[2]In practice, the computation tasks may have different numbers of bits. In this case, the approach proposed in this paper can still serve as an important reference to the computation tasks with different numbers of bits.

where $P_{c,i}$ is the accessible computational power at the CAP_i. Note that the first term in (5) and (6) is the latency and energy consumption of the communication from the source, while the second term is the latency and energy consumption of the computation at CAP_i.

III. A New Definition for Outage Probability in MEC Networks

In traditional communication-orientated networks, the outage is typically referred to the SNR outage at the receiver, which occurs when the received SNR falls below a given threshold. In contrast, in MEC networks, latency and energy consumption are the two most significant performance metrics [32]–[34]. Specifically, latency is particularly important in the cases of video transmission, navigation, and control-orientated systems, while energy consumption attracts broad interests since the MEC nodes are energy-aware, especially when they have limited energy. By taking into account the joint impact of latency and energy consumption, we define an outage event for MEC networks from the perspectives of both communication and computation. This event occurs when either the latency or the energy consumption is higher than certain thresholds. Accordingly, the new definition for the outage probability associated with the CAP_i is

$$P_{out,i} = \Pr[(t_i > \gamma_T) || (E_i > \gamma_E)], \tag{7}$$

where $||$ denotes the logical OR operation, and γ_T and γ_E are the thresholds of latency and energy consumption, respectively. Note that γ_T and γ_E are used to measure the system outage performance, and hence they are involved in the outage calculation of the following SC and SSC protocols. As indicated in (7), an outage event in MEC networks involves both latency and energy consumption.

IV. SC and SSC Protocols

In this section, we present two opportunistic CAP selection protocols for MEC networks, which can be used to select one MEC branch to assist the communication and computation.

A. SC Protocol

In the SC protocol, the CAP_i firstly estimates the channel parameter at the beginning of each transmission, assisted by pilot signals from the source S. Then, it computes the associated latency t_i and energy consumption E_i, by using (5) and (6). Based on t_i and E_i, the system forms the set,

$$\Omega = \{i = 1, 2 | \text{If } t_i \le \gamma_T \text{ and } E_i \le \gamma_E\}. \tag{8}$$

If Ω is not empty, the system further chooses the best MEC branch CAP_{i^*} among the set Ω, either by minimizing the latency or energy consumption,

$$i^* = \arg\min_{i \in \Omega} \theta_i, \tag{9}$$

where θ_i can be t_i or E_i. On the contrary, if Ω is empty, neither branch can satisfy the outage requirement and the outage event will occur. In this case, the system can choose not to communicate, or communicate by using a relatively better branch among the two branches through some criteria, such as minimizing the latency or energy consumption.

B. SSC Protocol

Although the SC protocol can always select the best branch to assist the communication and computation, it has several limitations in practice. First, it needs continuous estimation of the channel parameters of both branches for each task, which imposes a heavy load on system implementation. Second, it requires to compare the latency or energy consumption of two branches in order to choose the best one, which increases the implementation complexity. Third, it may result in a frequent node switching, which is harmful to the network stability.

To overcome such limitations of the SC protocol, the SSC protocol is employed for MEC networks. In the SSC protocol, only one MEC branch CAP_i ($i \in \{1, 2\}$) is activated to assist the communication and computation. The same MEC branch is continuously used, as long as it can support the communication and computation. Only when the branch cannot meet the requirements of latency and energy, a branch switching occurs and the other branch is activated. Let λ_T and λ_E represent the switching thresholds of latency and energy consumption in the SSC protocol, respectively. Accordingly, λ_T and λ_E are involved in the outage calculation of the SSC protocol, while not involved in the outage calculation of the SC protocol. Suppose that CAP_1 was used for the communication and computation of the previous task. Then, for the current task, the branch switching occurs if

$$t_1 > \lambda_T, \tag{10}$$

or

$$E_1 > \lambda_E. \tag{11}$$

This indicates that when either the latency is large or the energy consumption is high, a branch switching occurs, and the other MEC branch CAP_2 is activated. Note that the classical operation in the SSC protocol is to switch to the other branch when the branch switching occurs, without checking whether the switched branch can satisfy the outage requirement or not. This is reasonable because that the previous branch has already failed to satisfy the outage requirement, and the system has to switch to other branch. In this case, the outage may still occur when the switched branch cannot satisfy the outage requirement. In particular, if neither branch can satisfy the outage requirement, both SC and SSC protocols lead to an outage event. It is emphasized that the main target of using the SSC protocol is not to guarantee non-outage, but to reduce the implementation complexity of the SC protocol, while maintaining a certain level of the outage performance.

In the SC and SSC protocols, the two branches may have unbalanced traffic load when the associated statistical information is different, such as the average channel gain and the computational capability at the CAPs. This unbalance can be solved by imposing some weight coefficients on the latency and energy consumption of each branch, at the cost of some degradation in outage probability. The weight coefficients can adjust the traffic load between the two branches [35], [36], and help achieve the fairness between the two CAPs in the considered MEC network.

Moreover, from the above two branch selection schemes with RAS or MRC at the receiver, we can design the system flexibly in practice, by taking into account both the outage performance and implementation complexity. Specifically, if the system is sensitive to outage, the SC protocol with MRC can be used; while if the system is sensitive to the implementation complexity, the SSC protocol with RAS tends can used. Therefore, the work in this paper provides a flexible choice for the system design.

V. Outage Probability Analysis

A. SC Protocol

As described above in the SC protocol, an outage occurs when neither of the two CAPs can meet the requirements of latency and energy consumption. Accordingly, the outage probability of the SC protocol along with either RAS and MRC at the receiver is given by,

$$P_{out,\Xi}^{\mathcal{SC}} = \Pr[(t_1 > \gamma_T)||(E_1 > \gamma_E), (t_2 > \gamma_T)||(E_2 > \gamma_E)], \tag{12}$$

where the subscript Ξ can be either RAS and MRC, indicating that either the RAS or MRC operation is employed at the receiver, respectively.

Theorem 1: The outage probability of the SC protocol along with either RAS and MRC at the receiver is given by,

$$P_{out,\Xi}^{\mathcal{SC}} = \phi_{1,\Xi}(\gamma_T, \gamma_E)\phi_{2,\Xi}(\gamma_T, \gamma_E), \tag{13}$$

where

$$\phi_{i,RAS}(x,y) = \left(1 - \exp\Big(-\frac{m_i\sigma^2\gamma_{eq}(x,y)}{P_S\alpha_i}\Big) \times \sum_{k=0}^{m_i-1}\frac{1}{k!}\Big(-\frac{m_i\sigma^2\gamma_{eq}(x,y)}{P_S\alpha_i}\Big)^k\right)^K, \tag{14}$$

$$\phi_{i,MRC}(x,y) = 1 - \exp\Big(-\frac{m_i\sigma^2\gamma_{eq}(x,y)}{P_S\alpha_i}\Big) \times \sum_{k=0}^{m_iK-1}\frac{1}{k!}\Big(-\frac{m_i\sigma^2\gamma_{eq}(x,y)}{P_S\alpha_i}\Big)^k, \tag{15}$$

$$\gamma_{eq}(x,y) = 2^{\frac{L}{W_B d_i(x,y)}} - 1, \tag{16}$$

$$d_i(x,y) = \min\Big(x - \frac{\rho L}{f_i}, \frac{y - \rho L P_{c,i}/f_i}{P_S}\Big), \tag{17}$$

in which $\gamma_{eq}(x,y)$ denotes the equivalent SNR threshold taking into account the requirements of both communication and computation, and $d_i(x,y)$ represents the requirement of t_{i1} from the perspectives of both latency and energy consumption.

Proof: See Appendix A. ∎

In order to obtain some insights on the system design, next we analyze the impact of system parameters on the network outage probability. From the analytical expression of $\phi_{i,\Xi}(x,y)$, we can conclude that $\frac{\partial P_{out,\Xi}^{\mathcal{SC}}}{\partial L} > 0$ and $\frac{\partial P_{out,\Xi}^{\mathcal{SC}}}{\partial W_B} < 0$ hold. Moreover, $P_{out,\Xi}^{\mathcal{SC}}$ is also affected by the transmit power P_S. To study this impact, we first consider the MEC outage probability of a single branch CAP_i, $\phi_{i,\Xi}(\gamma_T, \gamma_E)$, and we use $P_{i,S}$ to denote the associated transmit power at the source.

The effect of $P_{i,S}$ on the MEC outage probability of a single branch is given by the following proposition,

Proposition 1: The partial derivative of the MEC outage probability of the i-th branch, $\phi_{i,\Xi}(\gamma_T, \gamma_E)$, with respect to the transmit power $P_{i,S}$, is given by,

$$\frac{\partial \phi_{i,\Xi}(\gamma_T,\gamma_E)}{\partial P_{i,S}} = \begin{cases} <0, & \text{If } P_{i,S} \in [0, P^*_{i,S}] \\ >0, & \text{Else} \end{cases}, \tag{18}$$

where $P^*_{i,S}$ is the optimal transmit power for the i-th MEC branch, given by

$$P^*_{i,S} = \frac{\gamma_E - \rho L P_{c,i}/f_i}{\gamma_T - \rho L/f_i}. \tag{19}$$

Proof: See Appendix B. ∎

To obtain more insights on the MEC networks with SC protocol, we further present some asymptotic expression for the outage probability in the low regime of noise power. By using the approximation of $e^x \simeq \sum_{n=0}^{N} \frac{x^n}{n!}$ for small value of $|x|$ [37], we can obtain the asymptotic $\phi_{i,\Xi}(x,y)$ after some manipulations as

$$\phi_{i,\Xi}(x,y) \simeq \mu_{i,\Xi}\Big(\frac{\sigma^2\gamma_{eq}(x,y)}{P_S\alpha_i}\Big)^{m_iK}, \tag{20}$$

where

$$\mu_{i,RAS} = \Big(\frac{m_i^{m_i-1}}{\Gamma(m_i)}\Big)^K, \tag{21}$$

$$\mu_{i,MRC} = \frac{m_i^{m_iK}}{\Gamma(m_iK+1)}. \tag{22}$$

From the asymptotic $\phi_{i,\Xi}(x,y)$, we can obtain the asymptotic outage probability of the MEC networks with SC protocol as

$$P^{\mathcal{SC}}_{out,\Xi} \simeq \frac{\mu_{1,\Xi}\mu_{2,\Xi}}{\alpha_1^{m_1K}\alpha_2^{m_2K}}\Big(\frac{\sigma^2\gamma_{eq}(\gamma_T,\gamma_E)}{P_S}\Big)^{(m_1+m_2)K}. \tag{23}$$

From Proposition 1 and the asymptotic $P^{\mathcal{SC}}_{out,\Xi}$, we can obtain some insights on the system design, as follow:

- The SC protocol can fully exploit the two branches in the MEC networks, and achieve the system full diversity order of $(m_1+m_2)K$. This indicates that the system performance can be rapidly improved by increasing the number of antennas at the CAPs and Nakagami parameters.
- The outage probability of MEC networks with SC protocol becomes worse with a larger L or smaller W_B, as more bits or narrower bandwidth will result in a larger latency and higher energy consumption.
- The optimal transmit power P^*_S is in the interval of $[P^*_{1,S}, P^*_{2,S}]$, where we assume that $P^*_{1,S} \le P^*_{2,S}$ without loss of generality. By analyzing the derivative of $\phi_{1,\Xi}(\gamma_T,\gamma_E)\phi_{2,\Xi}(\gamma_T,\gamma_E)$ with respect to P_S, we can readily obtain the value of P^*_S. In particular, when $P^*_{1,S} = P^*_{2,S}$ holds, the optimal transmit power P^*_S is equal to $P^*_{1,S}$.

B. SSC Protocol

According to the SSC protocol, the outage probability with RAS or MRC is given by

$$\begin{aligned} P^{\mathcal{SSC}}_{out,\Xi} &= \eta_{1,\Xi}\underbrace{\Pr[t_1 \le \lambda_T, E_1 \le \lambda_E, (t_1 > \gamma_T)||(E_1 > \gamma_E)]}_{J_{1,\Xi}} \\ &+ \eta_{1,\Xi}\underbrace{\Pr[(t_1 > \lambda_T)||(E_1 > \lambda_E), (t_2 > \gamma_T)||(E_2 > \gamma_E)]}_{J_{2,\Xi}} \\ &+ \eta_{2,\Xi}\underbrace{\Pr[t_2 \le \lambda_T, E_2 \le \lambda_E, (t_2 > \gamma_T)||(E_2 > \gamma_E)]}_{J_{3,\Xi}} \\ &+ \eta_{2,\Xi}\underbrace{\Pr[(t_2 > \lambda_T)||(E_2 > \lambda_E), (t_1 > \gamma_T)||(E_1 > \gamma_E)]}_{J_{4,\Xi}}, \end{aligned} \tag{24}$$

where $J_{1,\Xi}$ and $J_{3,\Xi}$ denote the outage probabilities when CAP_1 and CAP_2 are continuously used, respectively, while $J_{2,\Xi}$ and $J_{4,\Xi}$ represent the outage probabilities when the branch switching occurs from CAP_1 to CAP_2 and vice versa, respectively. Moreover, $\eta_{1,\Xi}$ and $\eta_{2,\Xi}$ are the probabilities that CAP_1 and CAP_2 are used, respectively, which are given by

$$\eta_{1,\Xi} = \frac{\Pr[(t_2 > \lambda_T)||(E_2 > \lambda_E)]}{\sum_{i=1}^{2}\Pr[(t_i > \lambda_T)||(E_i > \lambda_E)]}, \tag{25}$$

$$\eta_{2,\Xi} = \frac{\Pr[(t_1 > \lambda_T)||(E_1 > \lambda_E)]}{\sum_{i=1}^{2}\Pr[(t_i > \lambda_T)||(E_i > \lambda_E)]}. \tag{26}$$

Theorem 2: The outage probability of the SSC protocol is given by,

$$P^{\mathcal{SSC}}_{out,\Xi} = \eta_{1,\Xi}(J_{1,\Xi} + J_{2,\Xi}) + \eta_{2,\Xi}(J_{3,\Xi} + J_{4,\Xi}), \tag{27}$$

where

$$\eta_{1,\Xi} = \frac{\phi_{2,\Xi}(\lambda_T,\lambda_E)}{\sum_{i=1}^{2}\phi_{i,\Xi}(\lambda_T,\lambda_E)}, \tag{28}$$

$$\eta_{2,\Xi} = \frac{\phi_{1,\Xi}(\lambda_T,\lambda_E)}{\sum_{i=1}^{2}\phi_{i,\Xi}(\lambda_T,\lambda_E)}, \tag{29}$$

and $J_{1,\Xi}$ and $J_{3,\Xi}$ are given in (30) and (32), and

$$J_{2,\Xi} = \phi_{1,\Xi}(\lambda_T,\lambda_E)\phi_{2,\Xi}(\gamma_T,\gamma_E), \tag{31}$$

$$J_{4,\Xi} = \phi_{1,\Xi}(\gamma_T,\gamma_E)\phi_{2,\Xi}(\lambda_T,\lambda_E). \tag{33}$$

Proof: See Appendix C. ∎

We highlight that the derived analytical $P^{\mathcal{SSC}}_{out,\Xi}$ consists of elementary functions only, and hence we can easily evaluate the outage probability of the MEC networks.

Next, to obtain some useful insights on the system design, we analyze how the network outage probability depends on the switching thresholds λ_T and λ_E,

Proposition 2: The partial derivatives of $P^{\mathcal{SSC}}_{out,\Xi}$ with respect to the switching thresholds λ_T and λ_E are

$$\frac{\partial P^{\mathcal{SSC}}_{out,\Xi}}{\partial \lambda_T} = \begin{cases} \le 0, & \text{If } \lambda_T \in [0, \gamma_T] \\ \ge 0, & \text{Else} \end{cases}, \tag{34}$$

$$J_{1,\Xi}=\begin{cases}0, & \text{If } \lambda_T\in[0,\gamma_T),\lambda_E\in[0,\gamma_E)\\ \phi_{1,\Xi}(\lambda_T,\gamma_E)-\phi_{1,\Xi}(\lambda_T,\lambda_E), & \text{If } \lambda_T\in[0,\gamma_T),\lambda_E\in[\gamma_E,\infty)\\ \phi_{1,\Xi}(\gamma_T,\lambda_E)-\phi_{1,\Xi}(\lambda_T,\lambda_E), & \text{If } \lambda_T\in[\gamma_T,\infty),\lambda_E\in[0,\gamma_E)\\ \phi_{1,\Xi}(\gamma_T,\gamma_E)-\phi_{1,\Xi}(\lambda_T,\lambda_E), & \text{If } \lambda_T\in[\gamma_T,\infty),\lambda_E\in[\gamma_E,\infty)\end{cases}, \tag{30}$$

$$J_{3,\Xi}=\begin{cases}0, & \text{If } \lambda_T\in[0,\gamma_T),\lambda_E\in[0,\gamma_E)\\ \phi_{2,\Xi}(\lambda_T,\gamma_E)-\phi_{2,\Xi}(\lambda_T,\lambda_E), & \text{If } \lambda_T\in[0,\gamma_T),\lambda_E\in[\gamma_E,\infty)\\ \phi_{2,\Xi}(\gamma_T,\lambda_E)-\phi_{2,\Xi}(\lambda_T,\lambda_E), & \text{If } \lambda_T\in[\gamma_T,\infty),\lambda_E\in[0,\gamma_E)\\ \phi_{2,\Xi}(\gamma_T,\gamma_E)-\phi_{2,\Xi}(\lambda_T,\lambda_E), & \text{If } \lambda_T\in[\gamma_T,\infty),\lambda_E\in[\gamma_E,\infty)\end{cases}, \tag{32}$$

and

$$\frac{\partial P_{out,\Xi}^{\mathcal{SSC}}}{\partial\lambda_E}=\begin{cases}\leq 0, & \text{If } \lambda_E\in[0,\gamma_E]\\ \geq 0, & \text{Else}\end{cases}. \tag{35}$$

Proof: See Appendix D. ∎

To obtain more insights on the system with SSC protocol, we extend to provide the asymptotic outage probability with low region of noise power. From the result in (20), we can obtain the asymptotic expressions of $\eta_{1,\Xi}$ and $\eta_{2,\Xi}$ by considering the relationship between m_1 and m_2 as

$$\eta_{1,\Xi}^{asy}=\begin{cases}0, & \text{If } m_1<m_2\\ \frac{\alpha_2^{m_2K}}{\alpha_1^{m_1K}+\alpha_2^{m_2K}}, & \text{If } m_1=m_2\\ 1, & \text{If } m_1>m_2\end{cases}, \tag{36}$$

$$\eta_{2,\Xi}^{asy}=\begin{cases}1, & \text{If } m_1<m_2\\ \frac{\alpha_1^{m_1K}}{\alpha_1^{m_1K}+\alpha_2^{m_2K}}, & \text{If } m_1=m_2\\ 0, & \text{If } m_1>m_2\end{cases}. \tag{37}$$

In further, by applying the asymptotic $\phi_{i,\Xi}(x,y)$ of (20) into Theorem 2, we can obtain the asymptotic expressions of $J_{1,\Xi}$, $J_{2,\Xi}$, $J_{3,\Xi}$ and $J_{4,\Xi}$ as,

$$J_{1,\Xi}\simeq q_{1,\Xi}\Big(\frac{\sigma^2}{P_S}\Big)^{m_1K}, \tag{38}$$

$$J_{2,\Xi}\simeq q_{2,\Xi}\Big(\frac{\sigma^2}{P_S}\Big)^{(m_1+m_2)K}, \tag{39}$$

$$J_{3,\Xi}\simeq q_{3,\Xi}\Big(\frac{\sigma^2}{P_S}\Big)^{m_2K}, \tag{40}$$

$$J_{4,\Xi}\simeq q_{4,\Xi}\Big(\frac{\sigma^2}{P_S}\Big)^{(m_1+m_2)K}, \tag{41}$$

where $q_{1,\Xi}$ and $q_{3,\Xi}$ are given in (42) and (44), and $q_{2,\Xi}$ and $q_{4,\Xi}$ are given by

$$q_{2,\Xi}=\mu_{1,\Xi}\mu_{2,\Xi}\Big(\frac{\gamma_{eq}(\lambda_T,\lambda_E)}{\alpha_1}\Big)^{m_1K}\Big(\frac{\gamma_{eq}(\gamma_T,\gamma_E)}{\alpha_2}\Big)^{m_2K}, \tag{43}$$

$$q_{4,\Xi}=\mu_{1,\Xi}\mu_{2,\Xi}\Big(\frac{\gamma_{eq}(\gamma_T,\gamma_E)}{\alpha_1}\Big)^{m_1K}\Big(\frac{\gamma_{eq}(\lambda_T,\lambda_E)}{\alpha_2}\Big)^{m_2K}, \tag{45}$$

From the above asymptotic expressions, we can obtain the asymptotic outage probability for the MEC networks with SSC protocol as

$$P_{out,\Xi}^{\mathcal{SSC}}\simeq\Big(\eta_{1,\Xi}^{asy}q_{2,\Xi}+\eta_{2,\Xi}^{asy}q_{4,\Xi}\Big)\Big(\frac{\sigma^2}{P_S}\Big)^{(m_1+m_2)K}+\eta_{1,\Xi}^{asy}q_{1,\Xi}\Big(\frac{\sigma^2}{P_S}\Big)^{m_1K}+\eta_{3,\Xi}^{asy}q_{3,\Xi}\Big(\frac{\sigma^2}{P_S}\Big)^{m_2K}. \tag{46}$$

From Proposition 2 and the asymptotic $P_{out,\Xi}^{\mathcal{SSC}}$, we can obtain the following useful insights on the system design,

- The optimal switching thresholds of latency and energy consumption, denoted by λ_T^* and λ_E^*, are equal to γ_T and γ_E, respectively, which can minimize the value of $P_{out,\Xi}^{\mathcal{SSC}}$ to $\phi_{1,\Xi}(\gamma_T,\gamma_E)\phi_{2,\Xi}(\gamma_T,\gamma_E)$ and achieve the system full diversity order of $(m_1+m_2)K$.
- When the switching thresholds are small with $\lambda_T\in[0,\gamma_T]$ and $\lambda_E\in[0,\gamma_E]$, the system diversity order is $(m_1+m_2)K$. However, as $P_{out,\Xi}^{\mathcal{SSC}}$ becomes worse with smaller λ_T and λ_E, very small switching thresholds resulting in too frequent branch switching are however harmful to the network performance.
- When the switching thresholds are large with either $\lambda_T>\gamma_T$ or $\lambda_E>\gamma_E$, there exists a term in the outage probability associated with a single MEC branch, i.e., $\eta_{1,\Xi}^{asy}q_{1,\Xi}\Big(\frac{\sigma^2}{P_S}\Big)^{m_1K}+\eta_{3,\Xi}^{asy}q_{3,\Xi}\Big(\frac{\sigma^2}{P_S}\Big)^{m_2K}$, indicating that the two MEC branches cannot be fully exploited with large switching thresholds. Hence, the network performance will deteriorate if the MEC branch switching seldom occurs.
- Similar to the SC protocol, the SSC protocol becomes worse with larger L or smaller W_B. Moreover, the optimal value of P_S is in the interval of $[P_{1,S}^*,P_{2,S}^*]$, which can be readily obtained by analyzing the derivative of $P_{out,\Xi}^{\mathcal{SSC}}$ with respect to P_S.

VI. Simulations and Numerical Results

In this section, we present some numerical and simulation results to validate the proposed approach. The number of required CPU cycles for each bit is set to 10 with $\rho=10$, and the CPU-cycle frequencies at the two CAPs are set to $f_1=6$ GHz and $f_2=10$ GHz, respectively. In addition, the computational powers at the two CAPs are set to $P_{c,1}=0.5$w and $P_{c,2}=1$w, respectively. Moreover, the wireless channels from the source to the two CAPs experience Nakagami-m

$$q_{1,\Xi}=\begin{cases}0, & \text{If } \lambda_T\in[0,\gamma_T),\lambda_E\in[0,\gamma_E)\\ \frac{\mu_{1,\Xi}}{\alpha_1^{m_1K}}[(\gamma_{eq}(\lambda_T,\gamma_E))^{m_1K}-(\gamma_{eq}(\lambda_T,\lambda_E))^{m_1K}], & \text{If } \lambda_T\in[0,\gamma_T),\lambda_E\in[\gamma_E,\infty)\\ \frac{\mu_{1,\Xi}}{\alpha_1^{m_1K}}[(\gamma_{eq}(\gamma_T,\lambda_E))^{m_1K}-(\gamma_{eq}(\lambda_T,\lambda_E))^{m_1K}], & \text{If } \lambda_T\in[\gamma_T,\infty),\lambda_E\in[0,\gamma_E)\\ \frac{\mu_{1,\Xi}}{\alpha_1^{m_1K}}[(\gamma_{eq}(\gamma_T,\gamma_E))^{m_1K}-(\gamma_{eq}(\lambda_T,\lambda_E))^{m_1K}], & \text{If } \lambda_T\in[\gamma_T,\infty),\lambda_E\in[\gamma_E,\infty)\end{cases}, \tag{42}$$

$$q_{3,\Xi}=\begin{cases}0, & \text{If } \lambda_T\in[0,\gamma_T),\lambda_E\in[0,\gamma_E)\\ \frac{\mu_{2,\Xi}}{\alpha_2^{m_2K}}[(\gamma_{eq}(\lambda_T,\gamma_E))^{m_2K}-(\gamma_{eq}(\lambda_T,\lambda_E))^{m_2K}], & \text{If } \lambda_T\in[0,\gamma_T),\lambda_E\in[\gamma_E,\infty)\\ \frac{\mu_{2,\Xi}}{\alpha_2^{m_2K}}[(\gamma_{eq}(\gamma_T,\lambda_E))^{m_2K}-(\gamma_{eq}(\lambda_T,\lambda_E))^{m_2K}], & \text{If } \lambda_T\in[\gamma_T,\infty),\lambda_E\in[0,\gamma_E)\\ \frac{\mu_{2,\Xi}}{\alpha_2^{m_2K}}[(\gamma_{eq}(\gamma_T,\gamma_E))^{m_2K}-(\gamma_{eq}(\lambda_T,\lambda_E))^{m_2K}], & \text{If } \lambda_T\in[\gamma_T,\infty),\lambda_E\in[\gamma_E,\infty)\end{cases}, \tag{44}$$

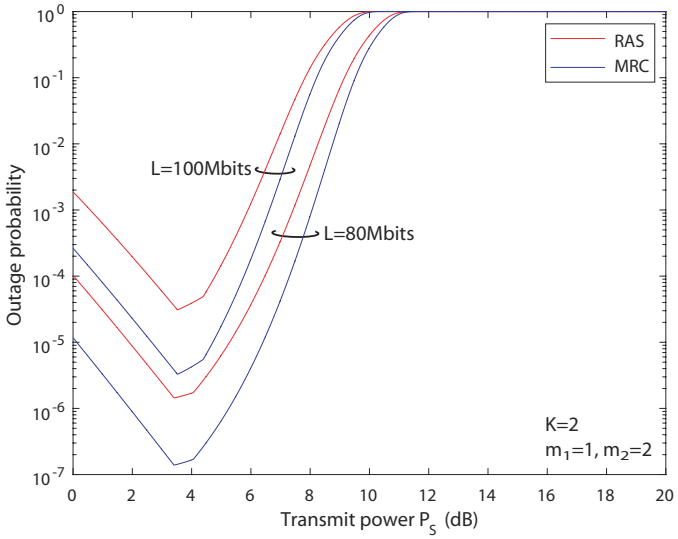

Fig. 2. Impact of transmit power P_S on the outage probability of SC-based MEC networks along with RAS and MRC.

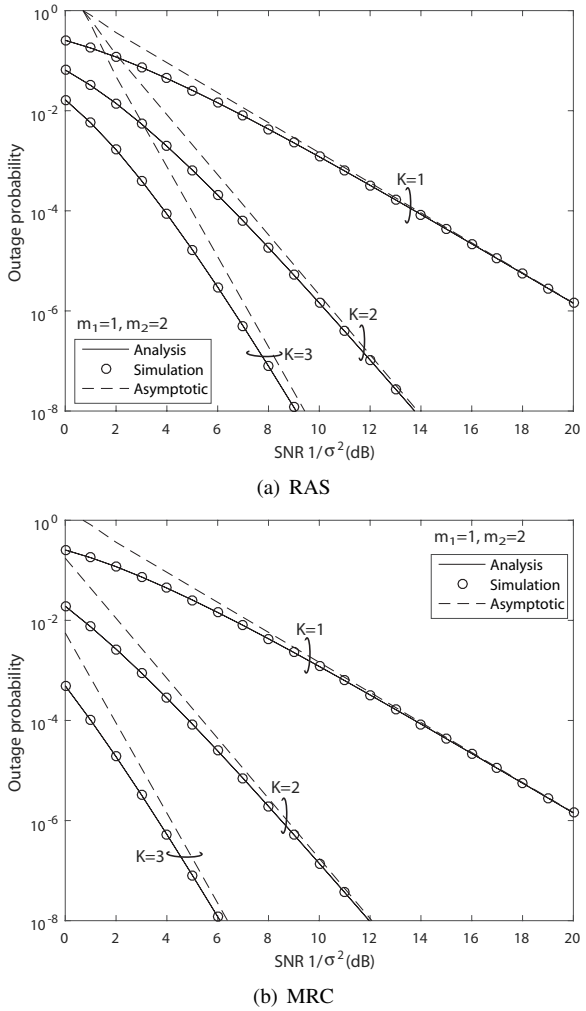

Fig. 3. Effect of number of transmit antenna on the outage probability of SC-based MEC networks versus SNR.

fading, where the channel bandwidth is set to 100 MHz, with $\alpha_1 = 3.5$ and $\alpha_2 = 1$. If not specified, the computation task has 80 Mbits, and the noise power of the AWGN at the CAPs is set to 0.1. In further, the thresholds of the latency and energy consumption are set to 0.5s and 1j, respectively.

Fig. 2 depicts the impact of the transmit power P_S on the analytical outage probability of the SC-based MEC networks along with RAS and MRC, where $K = 2$, $m_1 = 1$, $m_2 = 2$, L =80 or 100 Mbits and the transmit power P_S varies from 0 dB to 20 dB. It is evident from Fig. 2 that when the transmit power is low, the network outage probability improves with the increasing P_S, indicating that the transmission latency is the bottleneck of the system performance. In contrast, when the transmit power is high, the network outage probability deteriorates with the increasing P_S, as the transmission energy consumption becomes the bottleneck of the system performance. Overall, Fig. 2 shows that the optimal transmit power P_S^* should be a trade-off between the latency and energy consumption. Moreover, the network outage probability becomes worse with the increasing L, as a larger number of bits in the task increases both the latency and energy consumption. In further, the SC with MRC outperforms that with RAS, as the former utilizes all of the transmit antennas to send the task, which can help reduce both the transmission latency and energy consumption.

Figs. 3-4 illustrate the analytical, asymptotic and simulated outage probabilities of the SC-based MEC networks versus the SNR, where the value of SNR varies from 0dB to 20dB. Specifically, Fig. 3 shows the effect of the number of transmit

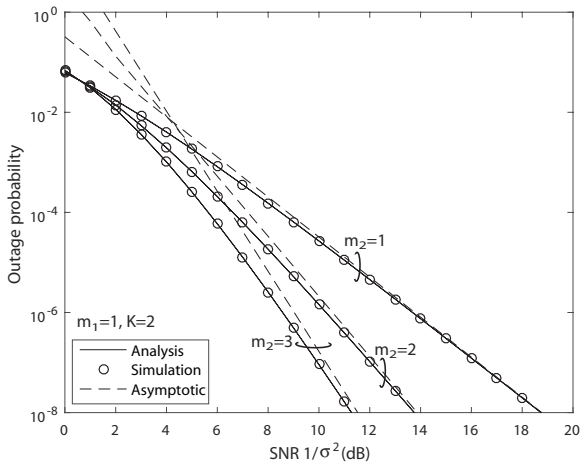

(a) RAS

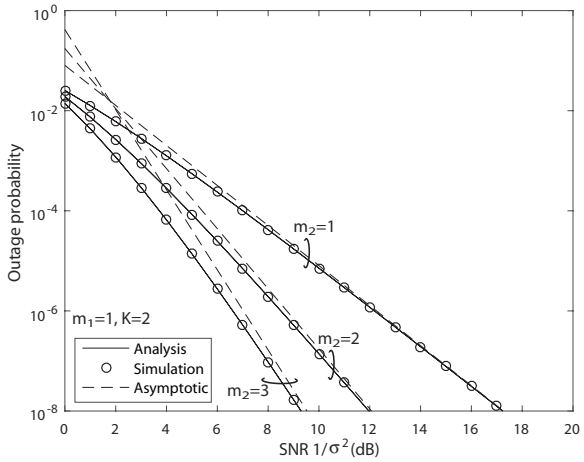

(b) MRC

Fig. 4. Effect of Nakagami parameter on the outage probability of SC-based MEC networks versus SNR.

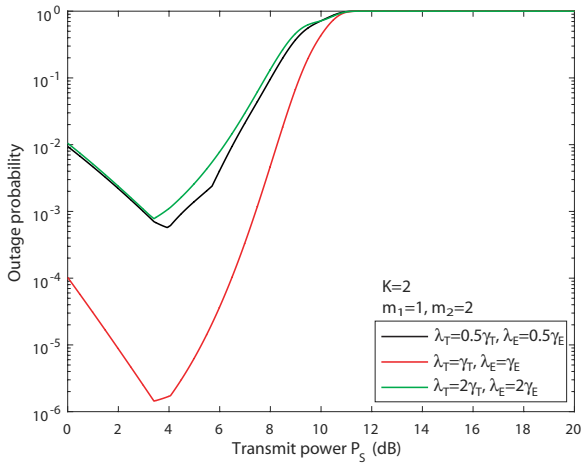

(a) RAS

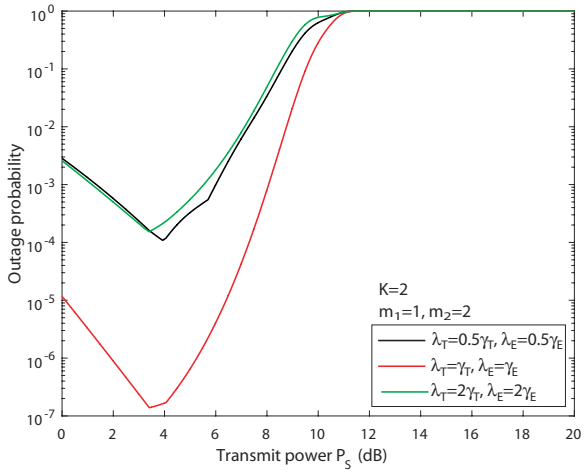

(b) MRC

Fig. 5. Impact of transmit power P_S on the outage probability of SSC-based MEC networks.

antenna with $m_1 = 1$, $m_2 = 2$, and $K \in \{1, 2, 3\}$, while Fig. 4 depicts the effect of the Nakagami parameter with $m_1 = 1$, $K = 2$, and $m_2 \in \{1, 2, 3\}$. In particular, Figs. 3-4 (a) and (b) correspond to RAS and MRC, respectively. Note that we use the optimal transmit power P_S^* in these two figures, and accordingly we define the SNR as $1/\sigma^2$ instead of P_S^*/σ^2 for the simplicity of measure. As observed from Figs. 3-4, we can see that for various values of SNR, K and m_2, the analytical outage probability matches well with the simulated one, which validates the effectiveness of the derived analytical expression of the outage probability for the SC-based MEC networks. Moreover, the asymptotic value converges to the exact one in the high SNR regime, which validates the asymptotic expression of the outage probability. In further, the network outage probability improves with the increasing K and m_2, since more antennas or larger Nakagami parameter can help enhance the wireless transmission, which reduces the transmission latency and energy consumption. In particular, the curve slope of the outage probability increases linearly with K and m_2, indicating that the system diversity order is proportional to the number of transmit antennas at the CAPs and the Nakagami parameter. Furthermore, we can find from Figs. 3-4 that the SC protocol with MRC outperforms that with RAS, indicating that the MRC can reduce the transmission latency and and the associated energy consumption at the cost of using all of transmit antennas.

Fig. 5 demonstrates the impact of transmit power on the analytical outage probability of the SSC-based MEC networks, where $L = 80$ Mbits, and the transmit power varies from 0 dB to 20 dB. Specifically, Fig. 5 (a) and (b) are associated with the RAS and MRC, respectively. To show the effect of the switching thresholds on the network outage probability, we use three different switching thresholds, i.e., $\lambda_T = \gamma_T$ and $\lambda_E = \gamma_E$, $\lambda_T = 2\gamma_T$ and $\lambda_E = 2\gamma_E$, and $\lambda_T = 0.5\gamma_T$ and $\lambda_E = 0.5\gamma_E$. As observed from this figure, we can see that for different switching thresholds, the network outage probability improves with the increasing P_S, in the low region of P_S. This is because that increasing the transmit power can help reduce the transmission latency. In contrast, when P_S is high, the network outage probability becomes worse with the increasing P_S, as a larger transmit power results in a higher energy consumption. Hence, the optimal value of the transmit power should be a trade-off between the transmission latency and energy consumption. Moreover, the SSC protocol with

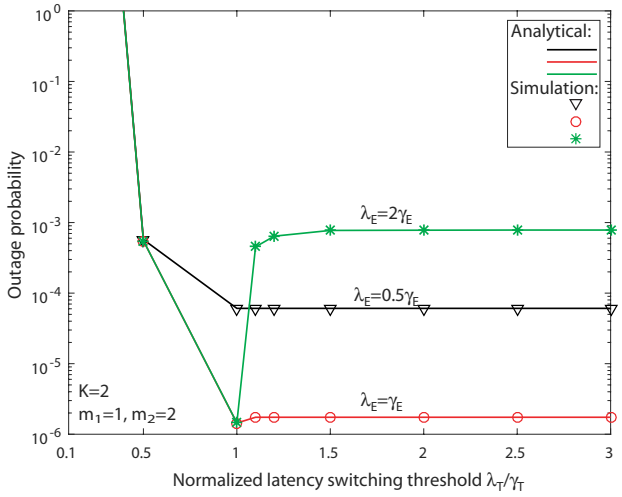

(a) RAS

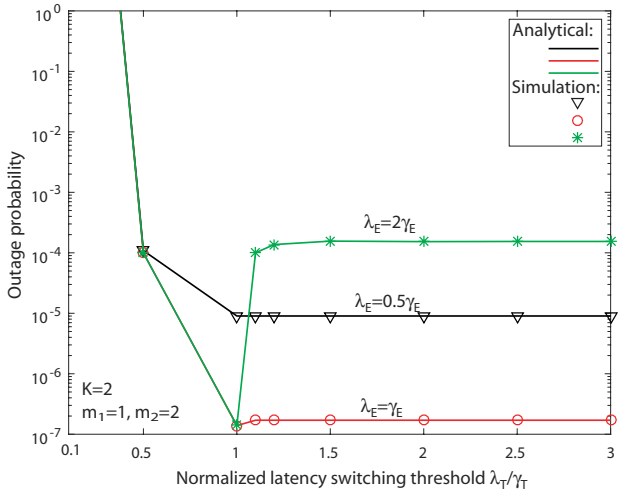

(b) MRC

Fig. 6. Effect of the normalized λ_T on the outage probability of SSC-based MEC networks.

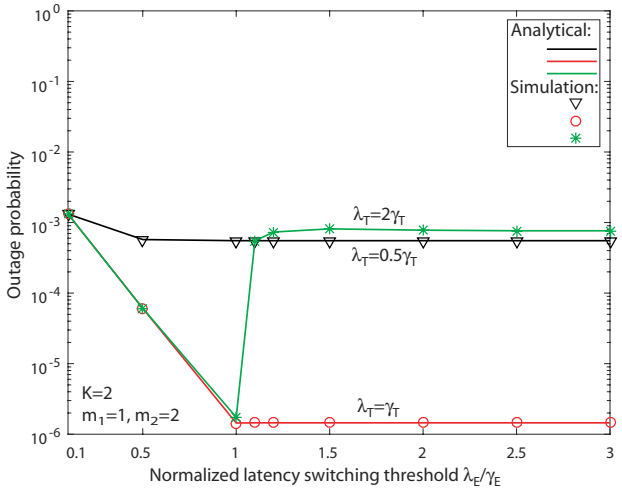

(a) RAS

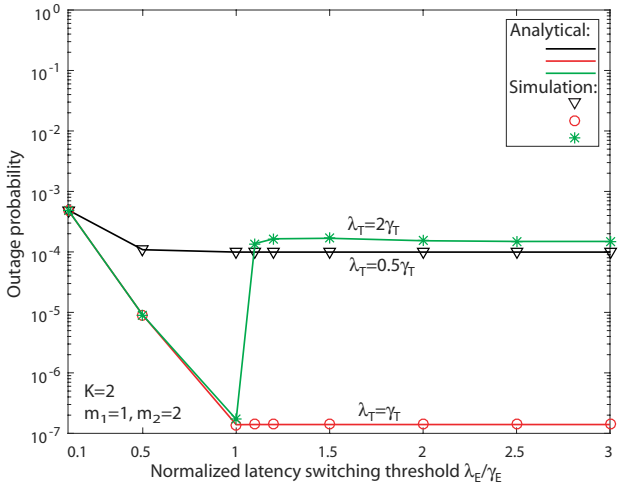

(b) MRC

Fig. 7. Effect of the normalized λ_E on the outage probability of SSC-based MEC networks.

$\lambda_T = \gamma_T$ and $\lambda_E = \gamma_E$ outperforms that with $\lambda_T = 2\gamma_T$ and $\lambda_E = 2\gamma_E$ or that with $\lambda_T = 0.5\gamma_T$ and $\lambda_E = 0.5\gamma_E$. This is because that SSC with $\lambda_T = 2\gamma_T$ and $\lambda_E = 2\gamma_E$ fails to exploit the two MEC branches effectively. In contrast, although SSC with $\lambda_T = 0.5\gamma_T$ and $\lambda_E = 0.5\gamma_E$ can exploit the two MEC branches, it leads to a frequent branch switching, causing its performance worse than that with $\lambda_T = \gamma_T$ and $\lambda_E = \gamma_E$.

Figs. 6-7 show how the analytical and simulated outage probabilities of the SSC-based MEC networks vary with the switching thresholds λ_T and λ_E, which are normalized by γ_T and γ_E, respectively. The optimal value of the transmit power P_S^* is used in these two figures, and Figs. 6-7 (a) and (b) correspond to the RAS and MRC, respectively. Specifically, Fig. 6 demonstrates the effect of the normalized λ_T with $\lambda_E \in \{0.5, 1, 2\}\gamma_E$, while Fig. 7 depicts the effect of the normalized λ_E with $\lambda_T \in \{0.5, 1, 2\}\gamma_T$. As observed from Fig. 6, we can find that for both RAS and MRC, when λ_T is small, SSC with $\lambda_E = 2\gamma_E$ has almost the same performance as SSC with $\lambda_E = \gamma_E$, as the latency becomes the main factor that determines the branch switching when the latency switching threshold is small. In contrast, when λ_T is large, the performances of the SSC with $\lambda_E = \gamma_E$ and SSC with $\lambda_E = 0.5\gamma_E$ remain almost unchanged with λ_T, since the energy consumption becomes the main factor that determines the branch switching when the latency switching threshold is large[3]. Moreover, the optimal switching thresholds λ_T^* and λ_E^* are equal to γ_T and γ_E, respectively. In further, the SSC with $\lambda_E = 2\gamma_E$ deteriorates very rapidly with the increasing λ_T, in the region of $\lambda_T \in [\gamma_T, \infty)$. This is because that large branch switching thresholds fail to exploit the two MEC branches effectively. Furthermore, the results in Fig. 7 demonstrate the similar phenomena as the results in Fig. 6. Finally, from the results in Figs. 6-7, we can conclude that for various values of λ_T and λ_E, the analytical outage probability is in good

[3]The impact of λ_T and λ_E on the SSC-based MEC networks is also evident from the expression of $\phi_{i,\Xi}(\lambda_T, \lambda_E)$. Specifically, when λ_T is small, $d_i(\lambda_T, \lambda_E)$ in $\phi_{i,\Xi}(\lambda_T, \lambda_E)$ becomes $\lambda_T - \rho L/f_i$, which is irrespective of λ_E. When λ_T is large, $d_i(\lambda_T, \lambda_E)$ becomes $\frac{\lambda_E - \rho L P_{c,i}/f_i}{P_S^*}$, which is irrespective of λ_T.

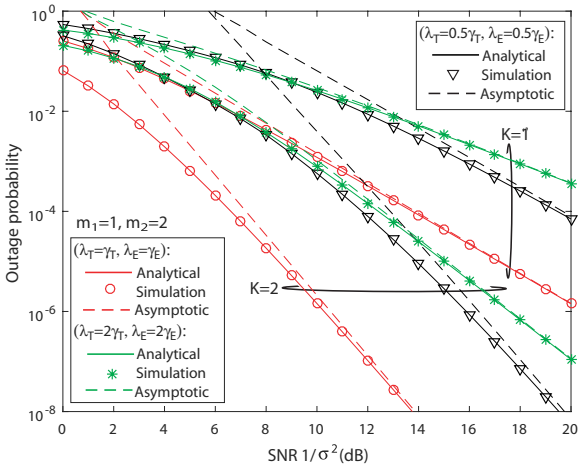

(a) RAS

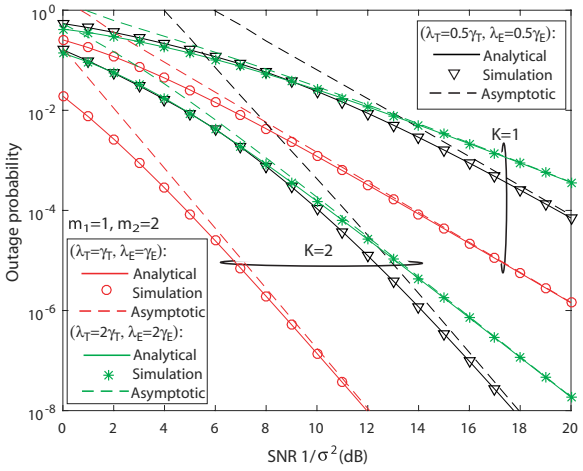

(b) MRC

Fig. 8. Effect of number of transmit antenna on the outage probability of SSC-based MEC networks versus SNR, with several branch switching thresholds.

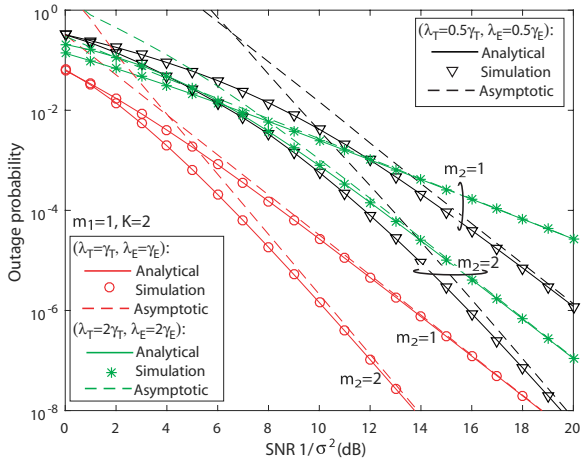

(a) RAS

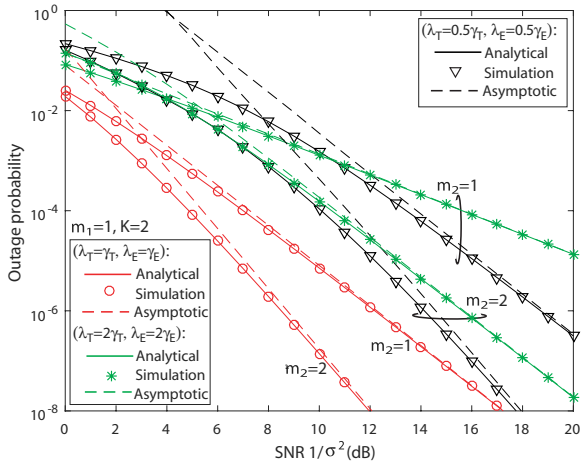

(b) MRC

Fig. 9. Effect of Nakagami parameter on the outage probability of SSC-based MEC networks versus SNR, with several branch switching thresholds.

agreement with the simulation one, which validates the derived analytical expression of the outage probability for the SSC-based MEC networks.

Figs. 8-9 show the analytical, asymptotic and simulated outage probabilities of the SSC-based MEC networks versus the SNR, where the optimal value of the transmit power is adopted and several branch switching thresholds are used with $\lambda_T = \gamma_T$ and $\lambda_E = \gamma_E$, $\lambda_T = 2\gamma_T$ and $\lambda_E = 2\gamma_E$, and $\lambda_T = 0.5\gamma_T$ and $\lambda_E = 0.5\gamma_E$. Specifically, Fig. 8 illustrates the effect of the number of transmit antenna with $m_1 = 1$, $m_2 = 2$, and $K = 1, 2$, while Fig. 9 depicts the effect of the Nakagami parameter with $m_1 = 1$, $K = 2$, and $m_2 = 1, 2$. In particular, Figs. 8-9 (a) and (b) correspond to the RAS and MRC, respectively. Note that we use the optimal transmit power P_S^* in these two figures. We can observe from these two figures that for various parameters including λ_T, λ_E, SNR, K and m_2, the analytical outage probability matches well with the simulated one, and the asymptotic value converges to the exact one when the SNR is high. This validates the derived analytical and asymptotic expressions for the outage probability of the SSC-based protocol. Moreover, the network outage probability becomes better when the value of K and m_2 increases, since more antennas or larger Nakagami parameter can help improve the wireless transmission, which decreases the transmission latency and energy consumption. In particular, the SSC protocol with $\lambda_T = \gamma_T$ and $\lambda_E = \gamma_E$ presents the curve slope of the outage probability linearly increasing with K and m_2, indicating that the SSC protocol can achieve the system full diversity order with proper branch switching thresholds. In contrast, the SSC protocol with $\lambda_T = 2\gamma_T$ and $\lambda_E = 2\gamma_E$ fails to achieve the same curve slope as the SSC protocol with $\lambda_T = \gamma_T$ and $\lambda_E = \gamma_E$, since large switching thresholds make the branch switching less happen. Furthermore, although the SSC protocol with $\lambda_T = 0.5\gamma_T$ and $\lambda_E = 0.5\gamma_E$ has the same curve slope as the SSC protocol with $\lambda_T = \gamma_T$ and $\lambda_E = \gamma_E$, its performance is worse. This is because that too frequent branch switching due to small switching thresholds is harmful to the network performance.

Fig. 10 compares the outage probabilities of the SC and SSC protocols for the MEC networks, where the optimal value of the transmit power is adopted and several branch switching thresholds are used with $\lambda_T = \gamma_T$ and $\lambda_E = \gamma_E$, $\lambda_T = 2\gamma_T$ and $\lambda_E = 2\gamma_E$, and $\lambda_T = 0.5\gamma_T$ and $\lambda_E = 0.5\gamma_E$.

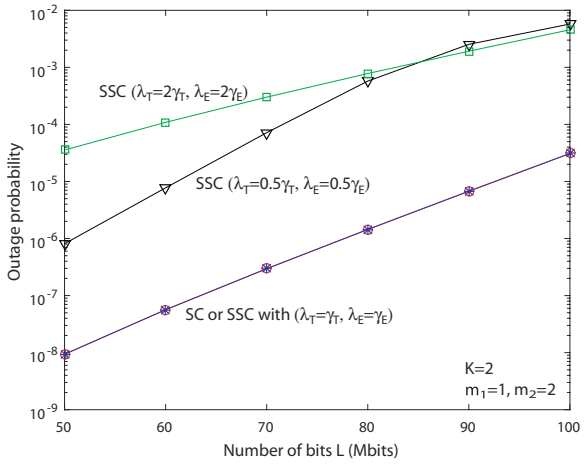

(a) RAS

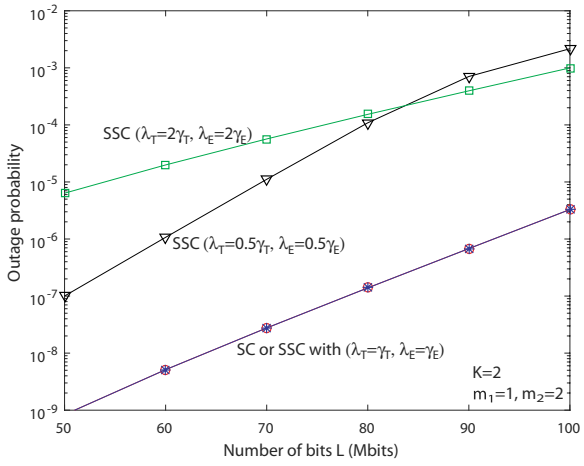

(b) MRC

Fig. 10. Performance comparison between SC and SSC protocols with several branch switching thresholds versus L.

Specifically, Fig. 10 (a) and (b) are associated with the RAS the MRC, respectively. We can find from Fig. 10 (a) and (b) that for various values of L and switching thresholds, the analytical outage probability fits well with the simulation one, which further verifies the effectiveness of the derived analytical expressions of the outage probability for the SC and SSC protocols. Moreover, the SC and SSC protocols improve with a smaller L, due to the reduced latency and energy consumption. In further, only the SSC protocol with the optimal switching threshold of $\lambda_T = \gamma_T$ and $\lambda_E = \gamma_E$ achieves the optimal outage probability of the SC protocol, while the SSC protocol with the other two switching thresholds fails to achieve, since the two MEC branches cannot be effectively exploited with either too large or too small branch switching thresholds. In particular, the SSC protocol with $\lambda_T = 0.5\gamma_T$ and $\lambda_E = 0.5\gamma_E$ is even worse than that with $\lambda_T = 2\gamma_T$ and $\lambda_E = 2\gamma_E$ when L is large. This is because that too large L increases the latency and energy consumption substantially, causing too frequent branch switching in the SSC protocol.

VII. Conclusions

This paper studied the MEC networks with two CAPs over Nakagami-m fading channels, where the CAPs were equipped with multiple antennas and one CAP was selected to accomplish the computation tasks from the source. To characterize the joint impact of communication and computation in MEC networks, a new form of outage probability was defined by taking into account both the latency and energy consumption. Then, RAS or MRC was utilized at the receiver, and SC or SSC protocol was employed to select one better CAP to accomplish the computation task. For both protocols, the analytical and asymptotic expressions of the outage probability were derived for the MEC networks. By analyzing how the outage probabilities varied with the system parameters, some important insights on the system design were obtained for the two protocols. Simulation and numerical results were finally illustrated to verify the proposed studies. In particular, the number of transmit antenna and Nakagami parameter could be exploited to reduce the latency and energy consumption rapidly, and the SSC protocol could achieve the same performance as the SC protocol with proper branch switching thresholds of latency and energy consumption.

Appendix A
Proof of Theorem 1

From (5) and (6), t_1 and E_1 contain the random variable (RV) u_1, while t_2 and E_2 contain the RV u_2. Since u_1 and u_2 are independent, we can rewrite $P_{out,\Xi}^{\mathcal{SC}}$ as

$$P_{out,\Xi}^{\mathcal{SC}} = \Pi_{i=1,2} \Pr[(t_i > \gamma_T)||(E_i > \gamma_E)]. \tag{A.1}$$

To facilitate the derivation process, we firstly derive a general function $\phi_{i,\Xi}(x,y)$, given by

$$\phi_{i,\Xi}(x,y) = \Pr[(t_i > x)||(E_i > y)], \tag{A.2}$$

which denotes the outage probability of the i-th MEC branch with a general latency threshold x and energy consumption threshold y. From (1)–(6), we can rewrite $\phi_{i,\Xi}(x,y)$ as

$$\phi_{i,\Xi}(x,y) = \Pr\left[\left(t_{i1} > x - \frac{\rho L}{f_i}\right)||\left(P_S t_{i1} > y - \frac{\rho L P_{c,i}}{f_i}\right)\right] \tag{A.3}$$

$$= \Pr\left[\left(t_{i1} > x - \frac{\rho L}{f_i}\right)||\left(t_{i1} > \frac{y - \rho L P_{c,i}/f_i}{P_S}\right)\right]. \tag{A.4}$$

Let $d_i(x,y)$ denote the requirement of t_{i1} from the perspectives of both latency and energy consumption, as shown in (17). Note that $d_i(x,y)$ contains determined variables only, and we can further write $\phi_{i,\Xi}(x,y)$ as,

$$\phi_{i,\Xi}(x,y) = \Pr(t_{i1} > d_i(x,y)) \tag{A.5}$$

$$= \Pr\left[\frac{L}{W_B \log_2(1 + \frac{P_S}{\sigma^2} u_i)} > d_i(x,y)\right] \tag{A.6}$$

$$= \Pr\left[u_i < \frac{\sigma^2}{P_S}\left(2^{\frac{L}{W_B d_i(x,y)}} - 1\right)\right]. \tag{A.7}$$

When the RAS is used at the receiver, the CDF of u_i can be written as

$$F_{u_i}(x) = \Pr\Big(\max_{1\le k\le K}|h_{i,k}|^2 < x\Big) \tag{A.8}$$

$$= \Big(\Pr(|h_{i,1}|^2 < x)\Big)^K. \tag{A.9}$$

By applying the PDF of $|h_{i,1}|^2$,

$$f_{|h_{i,1}|^2}(x) = \frac{m_i^{m_i}x^{m_i-1}}{\alpha_i^{m_i}\Gamma(m_i)}e^{-\frac{m_i x}{\alpha_i}}, \tag{A.10}$$

into (A.9), and then solving the required integral, we can obtain the analytical expression of $\phi_{i,\Xi}(x,y)$ with RAS, as shown in (14).

On the other hand, when the MRC is used at the receiver, the PDF of u_i is [31]

$$f_{u_i}(x) = \frac{(m_iK)^{m_iK}x^{m_iK-1}}{(K\alpha_i)^{m_iK}\Gamma(m_iK)}e^{-\frac{m_i x}{\alpha_i}}. \tag{A.11}$$

By applying (A.11) into (A.7), and then solving the required integral, we can obtain the analytical expression of $\phi_{i,\Xi}(x,y)$ with MRC, as shown in (15). From the analytical expression of $\phi_{i,\Xi}(x,y)$, we obtain the analytical outage probability of the MEC networks with SC protocol, as shown in Theorem 1. In this way, we have completed the proof of Theorem 1.

Appendix B
Proof of Proposition 1

According to the value of the transmit power $P_{i,S}$, we consider the two ranges of the transmit power, i.e., $P_{i,S}\in[0,P_{i,S}^*]$ and $P_{i,S}\in(P_{i,S}^*,\infty)$. In the first range of $P_{i,S}\in[0,P_{i,S}^*]$, $d_i(\gamma_T,\gamma_E)$ in $\phi_{i,\Xi}(\gamma_T,\gamma_E)$ becomes

$$d_i(\gamma_T,\gamma_E) = \gamma_T - \frac{\rho L}{f_i}. \tag{B.1}$$

By applying the above $d_i(\gamma_T,\gamma_E)$ into (14)-(15), we can find that $\frac{\partial\phi_{i,\Xi}(\gamma_T,\gamma_E)}{\partial P_{i,S}} < 0$ holds when $P_{i,S}\in[0,P_{i,S}^*]$.

In the second range of $P_{i,S}\in(P_{i,S}^*,\infty)$, $d_i(\gamma_T,\gamma_E)$ in $\phi_{i,\Xi}(\gamma_T,\gamma_E)$ becomes

$$d_i(\gamma_T,\gamma_E) = \frac{\gamma_E - \rho L P_{c,i}/f_i}{P_{i,S}}. \tag{B.2}$$

By applying the above $d_i(\gamma_T,\gamma_E)$ into (14)-(15), we can find that $\frac{\partial\phi_{i,\Xi}(\gamma_T,\gamma_E)}{\partial P_{i,S}} > 0$ holds when $P_{i,S}\in(P_{i,S}^*,\infty)$. In this way, the proof of Proposition 1 has been completed.

Appendix C
Proof of Theorem 2

From (14)-(15), we can write the analytical expressions of $\eta_{1,\Xi}$ and $\eta_{2,\Xi}$, as shown in (28)-(29). In further, from the analytical expression of $\phi_{i,\Xi}(x,y)$, we can write the analytical expressions of $J_{2,\Xi}$ and $J_{4,\Xi}$ in (24), as shown in (31) and (33).

We now extend to derive the analytical expressions of $J_{1,\Xi}$ and $J_{3,\Xi}$ in (24). The expression of $J_{1,\Xi}$ can be rewritten as

$$J_{1,\Xi} = \Pr(t_1\le\lambda_T, E_1\le\lambda_E) - \Pr[t_1\le\lambda_T, E_1\le\lambda_E, t_1\le\gamma_T, E_1\le\gamma_E] \tag{C.1}$$

$$= \Pr(t_1\le\lambda_T, E_1\le\lambda_E) - \Pr[t_1\le\min(\lambda_T,\gamma_T), E_1\le\min(\lambda_E,\gamma_E)]. \tag{C.2}$$

By considering that $\Pr(t_1\le\lambda_T, E_1\le\lambda_E) = 1-\Pr[(t_1>x)||(E_1>y)] = 1-\phi_{1,\Xi}(\lambda_T,\lambda_E)$, we can further write the analytical expression of $J_{1,\Xi}$ as

$$J_{1,\Xi} = \phi_{1,\Xi}[\min(\lambda_T,\gamma_T),\min(\lambda_E,\gamma_E)] - \phi_{1,\Xi}(\lambda_T,\lambda_E). \tag{C.3}$$

Similarly, the analytical expression of $J_{3,\Xi}$ is given by

$$J_{3,\Xi} = \phi_{2,\Xi}[\min(\lambda_T,\gamma_T),\min(\lambda_E,\gamma_E)] - \phi_{2,\Xi}(\lambda_T,\lambda_E). \tag{C.4}$$

In particular, by considering the relationship between λ_T and γ_T, and the relationship between λ_E and γ_E, we can specify the analytical expressions of $J_{1,\Xi}$ and $J_{3,\Xi}$ into four cases, shown in (30) and (32).

By summarizing the above analytical results of $\eta_{1,\Xi}$, $\eta_{2,\Xi}$, $J_{1,\Xi}$, $J_{2,\Xi}$, $J_{3,\Xi}$ and $J_{4,\Xi}$, we can obtain the analytical expression of outage probability for the SSC protocol for the considered MEC networks, as shown in (27). In this way, we have completed the proof of Theorem 2.

Appendix D
Proof of Proposition 2

To prove Proposition 2, we firstly divide the spaces spanned by the two switching thresholds λ_T and λ_E into four areas, $\mathcal{A}_1$, $\mathcal{A}_2$, $\mathcal{A}_3$ and $\mathcal{A}_4$, corresponding to $\lambda_T\in[0,\gamma_T]$ and $\lambda_E\in[0,\gamma_E]$, $\lambda_T\in(\gamma_T,\infty)$ and $\lambda_E\in(\gamma_E,\infty)$, $\lambda_T\in[0,\gamma_T]$ and $\lambda_E\in(\gamma_E,\infty)$, and $\lambda_T\in(\gamma_T,\infty)$ and $\lambda_E\in[0,\gamma_E]$, respectively. To simplify the notation, we omit the subscript Ξ in this part. We then consider the variation of $P_{out}^{\mathcal{SSC}}$ with respect to the switching thresholds λ_T and λ_E, in the four areas,

- $\mathcal{A}_1$: In this area, the analytical expression of $P_{out}^{\mathcal{SSC}}$ in (27) becomes,

$$P_{out}^{\mathcal{SSC}} = \eta_1\phi_1(\lambda_T,\lambda_E)\phi_2(\gamma_T,\gamma_E) + \eta_2\phi_1(\gamma_T,\gamma_E)\phi_2(\lambda_T,\lambda_E) \tag{D.1}$$

$$= \frac{v_1v_2}{v_1+v_2}(\phi_1+\phi_2) \tag{D.2}$$

$$= (\tilde{v}_1+\tilde{v}_2)^{-1}(\phi_1+\phi_2), \tag{D.3}$$

  where $v_i=\phi_i(\lambda_T,\lambda_E)$, and $\tilde{v}_i = 1/\phi_i(\lambda_T,\lambda_E)$ are used to simplify the derivation process for $i=1,2$. From (D.3), we can find that $\frac{\partial P_{out}^{\mathcal{SSC}}}{\partial\tilde{v}_i} < 0$ holds. Moreover, we can see from (14)-(17) that $\frac{\partial\tilde{v}_i}{\partial\lambda_T}\le 0$ and $\frac{\partial\tilde{v}_i}{\partial\lambda_E}\le 0$ hold. Hence, in the area of $\mathcal{A}_1$, $\frac{\partial P_{out}^{\mathcal{SSC}}}{\partial\lambda_T}\le 0$ and $\frac{\partial P_{out}^{\mathcal{SSC}}}{\partial\lambda_E}\le 0$ hold.
- $\mathcal{A}_2$: In this area, the analytical expression of $P_{out}^{\mathcal{SSC}}$ in (27) becomes,

$$P_{out}^{\mathcal{SSC}} = \eta_1(\phi_1-v_1) + \eta_2(\phi_2-v_2) + \eta_1v_1w_2 + \eta_2w_1v_2 \tag{D.4}$$

$$= \frac{v_1v_2}{v_1+v_2}\Big(\frac{w_1}{v_1}+\frac{w_2}{v_2}+w_1+w_2-2\Big) \tag{D.5}$$

$$= \frac{1}{\tilde{v}_1+\tilde{v}_2}(w_1\tilde{v}_1+w_2\tilde{v}_2+w_1+w_2-2). \tag{D.6}$$

Then, we take the partial derivative of $P_{out}^{\mathcal{SSC}}$ with respect to $\tilde{v}_1$ as

$$\frac{\partial P_{out}^{\mathcal{SSC}}}{\partial \tilde{v}_1} = \frac{1}{(\tilde{v}_1+\tilde{v}_2)^2}\Big[w_1(\tilde{v}_1+\tilde{v}_2) - (w_1\tilde{v}_1+w_2\tilde{v}_2+w_1+w_2-2)\Big] \tag{D.7}$$

$$= \frac{1}{(\tilde{v}_1+\tilde{v}_2)^2}(w_1\tilde{v}_2 - w_2\tilde{v}_2 + 2 - w_1 - w_2). \tag{D.8}$$

As $\phi_2(\lambda_T,\lambda_E) \leq \phi_2(\gamma_T,\gamma_E)$ holds for the area $\mathcal{A}_2$, we can obtain that $\tilde{v}_2 \geq \frac{1}{w_2}$. By applying this inequality into (D.8), we can further obtain that

$$\frac{\partial P_{out}^{\mathcal{SSC}}}{\partial \tilde{v}_1} \geq \frac{1}{(\tilde{v}_1+\tilde{v}_2)^2}\Big(\frac{w_1}{w_2} - w_2\tilde{v}_2 + 2 - w_1 - w_2\Big) \tag{D.9}$$

$$= \frac{1}{(\tilde{v}_1+\tilde{v}_2)^2}\frac{1}{w_2}[w_1 + 2w_2 - w_2(w_1+2w_2)] \tag{D.10}$$

$$> 0. \tag{D.11}$$

In a similar way, we can obtain that $\frac{\partial P_{out}^{\mathcal{SSC}}}{\partial \tilde{v}_2} > 0$ holds in the area $\mathcal{A}_2$. Moreover, it can be easily found that $\frac{\partial \tilde{v}_i}{\partial \lambda_T} \geq 0$ and $\frac{\partial \tilde{v}_i}{\partial \lambda_E} \geq 0$ hold for $i = 1, 2$. Hence, we can find that in the area $\mathcal{A}_2$, $\frac{\partial P_{out}^{\mathcal{SSC}}}{\partial \lambda_T} \geq 0$ and $\frac{\partial P_{out}^{\mathcal{SSC}}}{\partial \lambda_E} \geq 0$ hold.

- $\mathcal{A}_3$: In this area, the analytical expression of $P_{out}^{\mathcal{SSC}}$ in (27) becomes,

$$P_{out}^{\mathcal{SSC}} = \frac{1}{(\tilde{v}_1+\tilde{v}_2)}\Big[\tilde{v}_1\phi_1(\lambda_T,\gamma_E) + \tilde{v}_2\phi_2(\lambda_T,\gamma_E) + w_1 + w_2 - 2\Big]. \tag{D.12}$$

As only $\tilde{v}_1$ and $\tilde{v}_2$ depend on λ_E, while $\phi_i(\lambda_T,\gamma_E)$ does not depend on λ_E for $i = 1, 2$, we can refer to the steps in (D.7)–(D.11) and obtain that $\frac{\partial P_{out}^{\mathcal{SSC}}}{\partial \lambda_E} \geq 0$ holds in the area $\mathcal{A}_3$.

We now investigate $\frac{\partial P_{out}^{\mathcal{SSC}}}{\partial \lambda_T}$, by considering three ranges of γ_E, i.e., γ_E is large, small, or moderate. In the first case that γ_E is large, we have

$$\frac{\gamma_E - \rho L P_{c,i}/f_i}{P_S} \geq \lambda_T - \frac{\rho L}{f_i}. \tag{D.13}$$

Accordingly, we can obtain that $\phi_i(\lambda_T,\gamma_E) = \phi_i(\lambda_T,\lambda_E)$ for $i = 1, 2$. Then $P_{out}^{\mathcal{SSC}}$ in (D.12) becomes,

$$P_{out}^{\mathcal{SSC}} = \frac{1}{(\tilde{v}_1+\tilde{v}_2)}(w_1+w_2), \tag{D.14}$$

from which we can verify that $\frac{\partial P_{out}^{\mathcal{SSC}}}{\partial \lambda_T} < 0$ holds.

In the second case that γ_E is small, we have

$$\frac{\gamma_E - \rho L P_{c,i}/f_i}{P_S} < \lambda_T - \frac{\rho L}{f_i}. \tag{D.15}$$

Then, $d_i(\lambda_T,\gamma_E)$ in $\phi_i(\lambda_T,\gamma_E)$ and $d_i(\lambda_T,\lambda_E)$ in $\phi_i(\lambda_T,\lambda_E)$ both become $\frac{\gamma_E - \rho L P_{c,i}/f_i}{P_S}$, which does not depend on λ_T. Hence, we can obtain that $\frac{\partial P_{out}^{\mathcal{SSC}}}{\partial \lambda_T} = 0$ holds.

In the third case that γ_E is moderate, we have

$$\frac{\gamma_E - \rho L P_{c,i}/f_i}{P_S} < \lambda_T - \frac{\rho L}{f_i}, \tag{D.16}$$

and

$$\frac{\lambda_E - \rho L P_{c,i}/f_i}{P_S} \geq \lambda_T - \frac{\rho L}{f_i}. \tag{D.17}$$

In this situation, $\phi_1(\lambda_T,\gamma_E)$ is equal to $\phi_1(\gamma_T,\gamma_E)$, and $P_{out}^{\mathcal{SSC}}$ in (D.12) becomes,

$$P_{out}^{\mathcal{SSC}} = \frac{1}{(\tilde{v}_1+\tilde{v}_2)}(w_1\tilde{v}_1 + w_2\tilde{v}_2 + w_1 + w_2 - 2). \tag{D.18}$$

Similar to the steps in (D.7)–(D.11), we can find that $\frac{\partial P_{out}^{\mathcal{SSC}}}{\partial \lambda_T} \leq 0$ holds.

By summarizing the above three cases of γ_E, we can conclude that in the area $\mathcal{A}_3$, $\frac{\partial P_{out}^{\mathcal{SSC}}}{\partial \lambda_T} \leq 0$ and $\frac{\partial P_{out}^{\mathcal{SSC}}}{\partial \lambda_E} \geq 0$ hold.

- $\mathcal{A}_4$: By referring to the steps in the area $\mathcal{A}_3$, we can similarly find that in the area $\mathcal{A}_4$, $\frac{\partial P_{out}^{\mathcal{SSC}}}{\partial \lambda_T} \geq 0$ and $\frac{\partial P_{out}^{\mathcal{SSC}}}{\partial \lambda_E} \leq 0$ hold.

By summarizing the results in the above four areas of $\mathcal{A}_1$, $\mathcal{A}_2$, $\mathcal{A}_3$ and $\mathcal{A}_4$, we have completed the proof of Proposition 2.

REFERENCES

[1] L. Xiao, D. Jiang, D. Xu, H. Zhu, Y. Zhang, and H. V. Poor, "Two-dimensional antijamming mobile communication based on reinforcement learning," *IEEE Trans. Vehic. Tech.*, vol. 67, no. 10, pp. 9499–9512, 2018.

[2] L. Sun and H. Xu, "Unequal secrecy protection for untrusted two-way relaying systems: Constellation overlapping and noise aggregation," *IEEE Trans. Vehic. Tech.*, vol. 67, no. 10, pp. 9681–9695, 2018.

[3] L. Xiao, Y. Li, C. Dai, H. Dai, and H. V. Poor, "Reinforcement learning-based NOMA power allocation in the presence of smart jamming," *IEEE Trans. Vehic. Tech.*, vol. 67, no. 4, pp. 3377–3389, 2018.

[4] L. Sun and H. Xu, "Fountain-coding-based secure communications exploiting outage prediction and limited feedback," *IEEE Trans. Vehic. Tech.*, vol. 68, no. 1, pp. 740–753, 2019.

[5] L. Xiao, X. Wan, C. Dai, X. Du, X. Chen, and M. Guizani, "Security in mobile edge caching with reinforcement learning," *IEEE Wireless Commun.*, vol. 25, no. 3, pp. 116–122, 2018.

[6] J. Xu, L. Chen, and P. Zhou, "Joint service caching and task offloading for mobile edge computing in dense networks," in *IEEE Conference on Computer Communications (INFOCOM) Honolulu, HI, USA, April 16-19, 2018*, pp. 207–215.

[7] M. Liu and Y. Liu, "Price-based distributed offloading for mobile-edge computing with computation capacity constraints," *IEEE Wireless Commun. Lett.*, vol. 7, no. 3, pp. 420–423, 2018.

[8] Y. Zhang, X. Lan, Y. Li, L. Cai, and J. Pan, "Efficient computation resource management in mobile edge-cloud computing," *IEEE Internet of Things Journal*, vol. 6, no. 2, pp. 3455–3466, 2019.

[9] J. Zhao, Q. Li, and Y. Gong, "Computation offloading and resource allocation for mobile edge computing with multiple access points," *IET Commun.*, vol. PP, no. 99, pp. 1–10, 2019.

[10] J. Zhao, Q. Li, Y. Gong, and K. Zhang, "Computation offloading and resource allocation for cloud assisted mobile edge computing in vehicular networks," *IEEE Trans. Vehic. Tech.*, vol. 68, no. 8, pp. 7944–7956, 2019.

[11] X. Hu, L. Wang, K. Wong, M. Tao, Y. Zhang, and Z. Zheng, "Edge and central cloud computing: A perfect pairing for high energy efficiency and low-latency," *IEEE Trans. Wireless Commun.*, vol. 19, no. 2, pp. 1070–1083, 2020.

[12] H. Sun, F. Zhou, and R. Q. Hu, "Joint offloading and computation energy efficiency maximization in a mobile edge computing system," *IEEE Trans. Vehic. Tech.*, vol. 68, no. 3, pp. 3052–3056, 2019.

[13] F. Zhou, Y. Wu, R. Q. Hu, and Y. Qian, "Computation efficiency in a wireless-powered mobile edge computing network with NOMA," in *IEEE International Conference on Communications (ICC), Shanghai, China, May 20-24, 2019*, pp. 1–7.

[14] ——, "Computation rate maximization in UAV-enabled wireless-powered mobile-edge computing systems," *IEEE Journal on Selected Areas in Commun.*, vol. 36, no. 9, pp. 1927–1941, 2018.

[15] F. Zhou, H. Sun, Z. Chu, and R. Q. Hu, "Computation efficiency maximization for wireless-powered mobile edge computing," in *IEEE Global Communications Conference (GLOBECOM), Abu Dhabi, United Arab Emirates, December 9-13, 2018*, pp. 1–6.

[16] F. Wang, J. Xu, X. Wang, and S. Cui, "Joint offloading and computing optimization in wireless powered mobile-edge computing systems," *IEEE Trans. Wireless Commun.*, vol. 17, no. 3, pp. 1784–1797, 2018.

[17] X. Hu, K. Wong, and K. Yang, "Wireless powered cooperation-assisted mobile edge computing," *IEEE Trans. Wireless Commun.*, vol. 17, no. 4, pp. 2375–2388, 2018.

[18] F. Wang, J. Xu, and Z. Ding, "Multi-antenna NOMA for computation offloading in multiuser mobile edge computing systems," *IEEE Trans. Commun.*, vol. 67, no. 3, pp. 2450–2463, 2019.

[19] Z. Ding, P. Fan, and H. V. Poor, "Impact of non-orthogonal multiple access on the offloading of mobile edge computing," *IEEE Trans. Commun.*, vol. 67, no. 1, pp. 375–390, 2019.

[20] Y. He, F. R. Yu, N. Zhao, and H. Yin, "Secure social networks in 5G systems with mobile edge computing, caching, and device-to-device communications," *IEEE Wireless Commun.*, vol. 25, no. 3, pp. 103–109, 2018.

[21] F. S. Al-Qahtani, C. Zhong, and H. M. Alnuweiri, "Opportunistic relay selection for secrecy enhancement in cooperative networks," *IEEE Trans. Commun.*, vol. 63, no. 5, pp. 1756–1770, 2015.

[22] J. Tang, D. K. C. So, A. Shojaeifard, K. Wong, and J. Wen, "Joint antenna selection and spatial switching for energy efficient MIMO SWIPT system," *IEEE Trans. Wireless Commun.*, vol. 16, no. 7, pp. 4754–4769, 2017.

[23] L. Fan, N. Zhao, X. Lei, Q. Chen, N. Yang, and G. K. Karagiannidis, "Outage probability and optimal cache placement for multiple amplify-and-forward relay networks," *IEEE Trans. Vehic. Tech.*, vol. 67, no. 12, pp. 12 373–12 378, 2018.

[24] F. Zhang, Y. Zhang, W. Q. Malik, B. Allen, and D. J. Edwards, "Optimum receive antenna selection for transmit cyclic delay diversity," in *Proceedings of IEEE International Conference on Communications, ICC 2008, Beijing, China, 19-23 May 2008*, 2008, pp. 3829–3833.

[25] C. Zhong and T. Ratnarajah, "Performance of user selection in cognitive broadcast channels," *IEEE Trans. Commun.*, vol. 60, no. 12, pp. 3529–3534, 2012.

[26] D. S. Michalopoulos and G. K. Karagiannidis, "Distributed switch and stay combining (DSSC) with a single decode and forward relay," *IEEE Commun. Lett.*, vol. 11, no. 5, pp. 408–410, May 2007.

[27] ——, "Two-relay distributed switch and stay combining," *IEEE Trans. Commun.*, vol. 56, no. 11, pp. 1790–1794, Nov. 2008.

[28] L. Fan, S. Zhang, T. Q. Duong, and G. K. Karagiannidis, "Secure switch-and-stay combining (SSSC) for cognitive relay networks," *IEEE Trans. Commun.*, vol. 64, no. 1, pp. 70–82, 2016.

[29] L. Fan, X. Lei, R. Q. Hu, and S. Zhang, "Distributed two-way switch and stay combining with a single amplify-and-forward relay," *IEEE Wireless Commun. Lett.*, vol. 2, no. 4, pp. 379–382, 2013.

[30] X. Lai, L. Fan, X. Lei, J. Li, N. Yang, and G. K. Karagiannidis, "Distributed secure switch-and-stay combining over correlated fading channels," *IEEE Trans. Information Forensics and Security*, vol. 14, no. 8, pp. 2088–2101, August 2019.

[31] M. K. Simon and M. S. Alouini, *Digital Communication over Fading Channels*, 2nd ed. John Wiley, 2005.

[32] Z. Zhao, "A novel framework of three-hierarchical offloading optimization for MEC in industrial IoT networks," *IEEE Trans. Industrial Informatics*, vol. PP, no. 99, pp. 1–12, 2019.

[33] S. Bi and Y. J. Zhang, "Computation rate maximization for wireless powered mobile-edge computing with binary computation offloading," *IEEE Trans. Wireless Commun.*, vol. 17, no. 6, pp. 4177–4190, 2018.

[34] S. Bi and Y. A. Zhang, "An ADMM based method for computation rate maximization in wireless powered mobile-edge computing networks," in *IEEE International Conference on Communications (ICC), Kansas City, MO, USA, May 20-24, 2018*, pp. 1–7.

[35] D. S. Michalopoulos and G. K. Karagiannidis, "Phy-layer fairness in amplify and forward cooperative diversity systems," *IEEE Trans. Wireless Commun.*, vol. 7, no. 3, pp. 1073–1082, 2008.

[36] M. Sadeghi and A. M. Rabiei, "A fair relay selection scheme for a DF cooperative network with spatially random relays," *IEEE Trans. Vehic. Tech.*, vol. 66, no. 12, pp. 11 098–11 107, 2017.

[37] I. S. Gradshteyn and I. M. Ryzhik, *Table of Integrals, Series, and Products*, 7th ed. San Diego, CA: Academic, 2007.